The Company of **Biologists**

RESEARCH ARTICLE

Osteocrin, a peptide secreted from the heart and other tissues, contributes to cranial osteogenesis and chondrogenesis in zebrafish

Ayano Chiba[1], Haruko Watanabe-Takano[1], Kenta Terai[2], Hajime Fukui[1], Takahiro Miyazaki[1], Mami Uemura[2], Hisashi Hashimoto[3,4], Masahiko Hibi[3,4], Shigetomo Fukuhara[5] and Naoki Mochizuki[1,6,*]

ABSTRACT

The heart is an endocrine organ, as cardiomyocytes (CMs) secrete natriuretic peptide (NP) hormones. Since the discovery of NPs, no other peptide hormones that affect remote organs have been identified from the heart. We identified osteocrin (Ostn) as an osteogenesis/chondrogenesis regulatory hormone secreted from CMs in zebrafish. *ostn* mutant larvae exhibit impaired membranous and chondral bone formation. The impaired bones were recovered by CM-specific overexpression of OSTN. We analyzed the parasphenoid (ps) as a representative of membranous bones. In the shortened ps of *ostn* morphants, nuclear Yap1/Wwtr1-dependent transcription was increased, suggesting that Ostn might induce the nuclear export of Yap1/Wwtr1 in osteoblasts. Although OSTN is proposed to bind to NPR3 (clearance receptor for NPs) to enhance the binding of NPs to NPR1 or NPR2, OSTN enhanced C-type NP (CNP)-dependent nuclear export of YAP1/WWTR1 of cultured mouse osteoblasts stimulated with saturable CNP. OSTN might therefore activate unidentified receptors that augment protein kinase G signaling mediated by a CNP-NPR2 signaling axis. These data demonstrate that Ostn secreted from the heart contributes to bone formation as an endocrine hormone.

KEY WORDS: Osteocrin, Heart, Peptide, Osteogenesis, Chondrogenesis, Nppa, Nppb, Nppc

INTRODUCTION

The heart is not only an essential pump for circulation but also an endocrine organ that secretes natriuretic peptide (NP) hormones, including atrial natriuretic peptide (ANP; also known as NPPA) and brain (B-type) natriuretic peptide (BNP; also known as NPPB) (Ogawa and de Bold, 2014). Cardiomyocytes (CMs) secrete vascular endothelial growth factor A and angiopoietin 1 to direct coronary vascular development in a paracrine-dependent manner by

[1]Department of Cell Biology, National Cerebral and Cardiovascular Center Research Institute, 5-7-1 Fujishirodai, Suita, Osaka 565-8565, Japan. [2]Laboratory of Function and Morphology, Institute of Molecular and Cellular Biosciences, University of Tokyo, 1-1-1 Yayoi, Bunkyo-ku, Tokyo 113-0032, Japan. [3]Laboratory of Organogenesis and Organ Function, Bioscience and Biotechnology Center, Nagoya University, Furo-cho, Chigusa-ku, Nagoya, Aichi 464-8061, Japan. [4]Devision of Biological Science, Graduate School of Science Nagoya, Nagoya University, Furo-cho, Chigusa-ku, Nagoya, Aichi 464-8061, Japan. [5]Department of Molecular Pathophysiology, Institute of Advanced Medical Science, Nippon Medical School, 1-396 Kosugi-machi, Nakahara-ku, Kawasaki, Kanagawa 211-8533, Japan. [6]AMED-CREST, National Cerebral and Cardiovascular Center Research Institute, 5-7-1 Fujishirodai, Suita, Osaka 565-8565, Japan.

*Author for correspondence (nmochizu@ri.ncvc.go.jp)

(iD) N.M., 0000-0002-3938-9602

acting on endothelial cells during cardiogenesis (Arita et al., 2014; Riley and Smart, 2011). Therefore, CMs have the potential to secrete functional peptides, although the main function of CMs is in cardiac muscle contraction. Besides ANP and BNP, no other secretory peptides that function as endocrine hormones have been reported.

The NP family consists of ANP, BNP and C-type NP (CNP; also known as NPPC). These NPs bind to the NPR1, NPR2 and NPR3 family of transmembrane receptors. NPR1 and NPR2 have a guanylate cyclase domain, whereas NPR3 does not. NPR3 functions as a clearance receptor for ANP and BNP or as a Gi-activating receptor (Potter et al., 2006). ANP induces natriuresis in the kidney and relaxation of smooth muscle via NPR1 and NPR2. ANP exerts paracrine/autocrine roles on CMs in the heart, as ANP has recently been reported to regulate CM proliferation in zebrafish (Becker et al., 2014). In contrast to ANP and BNP, CNP is produced in a variety of tissues and organs including the uterus, ovarium, cartilaginous tissues, blood vessels and osteoblasts (Hagiwara et al., 1994; Stepan et al., 1999, 2002; Suda et al., 1996). It characteristically elongates long bones through NPR2 expressed on chondrocytes. The physiological relevance of CNP-NPR2 signaling to bone formation is apparent because *Cnp* (*Nppc*) knockout mice and *Npr2* knockout mice exhibit dwarfism (Komatsu et al., 2002; Tamura et al., 2004). Conversely, the forced expression of CNP and the depletion of *Npr3* result in increased bone length in mice (Dauphinee et al., 2013; Kake et al., 2009; Matsukawa et al., 1999).

Bone growth depends on endochondral ossification and intramembranous ossification (Karsenty et al., 2009). The former occurs during growth of the long bones, whereas the latter is found in the calvaria and clavicle. The chondrocyte lineage cells – prechondrogenic cells, proliferating chondrocytes, prehypertrophic chondrocytes and hypertrophic chondrocytes – participating in endochondral ossification respond to BNP and CNP because they express NPR2 receptors (Suda et al., 1998; Yasoda et al., 2004). Therefore, enhancement of BNP/CNP-NPR2 signaling results in the extension of long bones. During intramembranous ossification, osteoblasts differentiated from mesenchymal stem cells (MSCs) proliferate and secrete bone matrix, thereby contributing to bone formation in a manner that is independent of chondrocytes (Soltanoff et al., 2009).

Osteocrin (OSTN) is proposed to belong to the NP family as there are similarities in amino acid sequence (Moffatt and Thomas, 2009; Potter et al., 2006). OSTN and musclin were originally identified by signal-sequence trap methods as the same molecule from bone and muscle, respectively (Nishizawa et al., 2004; Thomas et al., 2003). The C-terminus of OSTN seems to be cleaved at 76KKKR79 and 110KKR112 sites. The resulting two fragments OSTN80-109 and OSTN113-130 have amino acid homology to NPs (Moffatt and Thomas, 2009), although neither fragment has the Cys-Cys

DEVELOPMENT

signature that is conserved in NPs and is essential for their circular structure. Nonetheless, OSTN is capable of binding to NPR3, thereby hampering the NP clearance activity of NPR3 (Thomas et al., 2003). Consistent with these findings, *Ostn* transgenic (Tg) mice exhibit extended long bones and kyphosis, presumably owing to the activation of NPR2 found in *Bnp* (*Nppb*) Tg mice (Suda et al., 1998; Thomas et al., 2003). The physiological role of OSTN in osteogenesis remains unclear, although it has been shown utilizing *Ostn* knockout mice to function as a myokine (Subbotina et al., 2015).

In this study, we aimed to search for secretory peptides from CMs of zebrafish and identified Ostn derived from the heart as an endocrine regulator for bone and cartilage. Ostn depletion led to shortening of the parasphenoid (ps), which is regulated by intramembranous ossification, and of the palatoquadrate (pq), which is regulated by chondrogenesis, while Ostn overexpression resulted in elongation of ps and pq. We further investigated how Ostn regulates ps formation, and found that Ostn regulates bone/cartilage formation by modifying CNP-dependent nuclear export of the transcriptional co-factors Yap1 and Wwtr1.

RESULTS

Ostn is expressed in CMs

ANP and BNP produced in the heart induce natriuresis through activation of NP receptors expressed in the renal tubules. Thus, the heart is thought to be an endocrine organ. First, we searched for secretory peptides produced from the heart. To obtain only CMs from the heart, we established two Tg zebrafish (*Danio rerio*) lines: *Tg(myl7:NLS-mCherry)* and *Tg(myl7:actn2-tdEos)* (Fig. 1A,C, Movies 1 and 2). Both the nuclear localization signal (NLS)-tagged monomeric (m)Cherry and actinin alpha 2 (Actn2)-tandem (td) Eos were seen to be exclusively expressed in the CMs using the *cardiac myosin light chain* (*myl7*) promoter when we carefully observed the fluorescence in heart by lightsheet and confocal microscopy. We isolated CMs from the hearts of these two Tg lines by fluorescence-activated cell sorting (FACS). *ostn* mRNA was expressed in the CMs of larvae of both Tg lines at 72 h post-fertilization (hpf) (Fig. 1B,D). The expression of mRNAs from the CMs was validated by the expression of *nppa*, *myl7* and *actc1a*. Moreover, genes known to be expressed in CMs, including *angpt1*, *bmp1a* and *epo*, were detected by RNA-seq (Fig. 1B,D).

We then examined the expression of *ostn* mRNA by whole-mount *in situ* hybridization (WISH) of larvae at 72 hpf. *ostn* mRNA was detected in the heart, corpuscles of Stannius (CS) and head (Fig. 2A). *ostn* mRNA was expressed in the heart where *myl7* mRNA was detected. Moreover, the expression of *ostn* mRNA seemed to be greater in the ventricle than in the atrium (Fig. 2B). The expression of *ostn* mRNA in the CS was confirmed by WISH of *calcium-sensing receptor* (*casr*) (Lin et al., 2014). Although *ostn* mRNA was exclusively expressed in the heart and CS at 36 hpf, it began to be detected in the head at 72 hpf (Fig. 2B). We examined in detail this expression in the head in brain sections to see whether it overlaps with that of myocytes (*myod1*), osteoblasts (*sp7*) and chondrocytes (*sox9a*). We found no clear overlap between *ostn* expression and these marker genes (Fig. S1). In addition, we investigated *Ostn* expression in adult mice (*Mus musculus*) and embryos by reverse transcription (RT)-PCR. *Ostn* mRNAs were mainly expressed in bones and muscles in adult mice, whereas subtle expression was detected in both atrium and ventricle of the embryonic mouse heart (Fig. S2A,B). These data suggest the possibility that Ostn secreted from CMs of zebrafish might function as a hormone that affects remote organs, including bones during early embryogenesis, just as mouse OSTN affects bone formation (Moffatt et al., 2007).
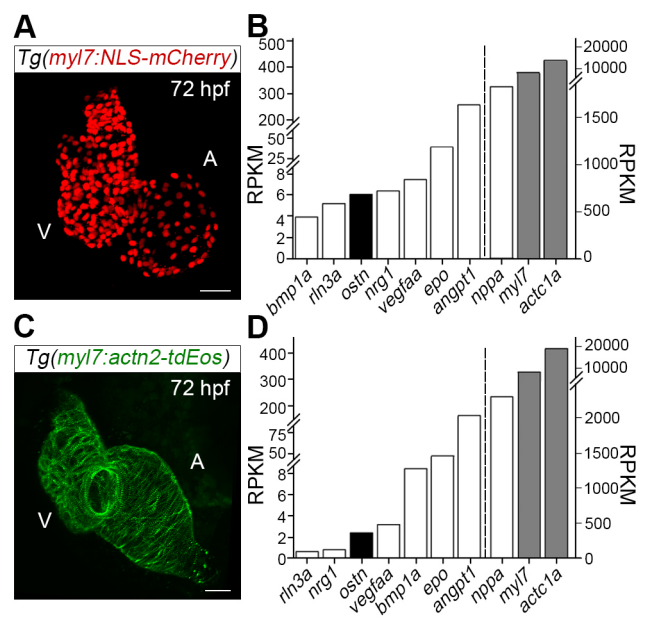

Fig. 1. Osteocrin (Ostn) is produced in cardiomyocytes of zebrafish. (A) Projection view of confocal images of the *Tg(myl7:NLS-mCherry)* heart at 72 hpf. A, atrium; V, ventricle. (B) RNA-seq analyses of mCherry-positive cardiomyocytes (CMs) from the hearts of *Tg(myl7:NLS-mCherry)* larvae at 72 hpf. Left and right y-axes report RPKM (reads per kilobase per million sequenced reads) values for the secretory molecules (left of the dashed line) and positive controls (right of the dashed line), respectively. Gray bars are used for structural proteins, white bars for secretory molecules. (C) Projection view of confocal images of the *Tg(myl7:actn2-tdEos)* heart at 72 hpf. (D) RNA-seq analyses of tdEos-positive CMs of *Tg(myl7:actn2-tdEos)*. Axes descriptions as in B. Scale bars: 30 μm.

Ostn derived from CMs contributes to membranous bone formation

To study the function of Ostn in zebrafish osteogenesis, we developed *ostn* knockout fish using transcription activator-like effector nuclease (TALEN). TALEN targeting to *ostn* successfully
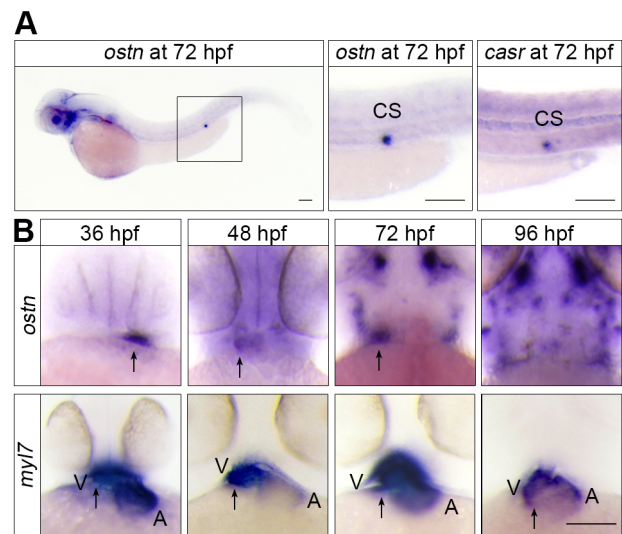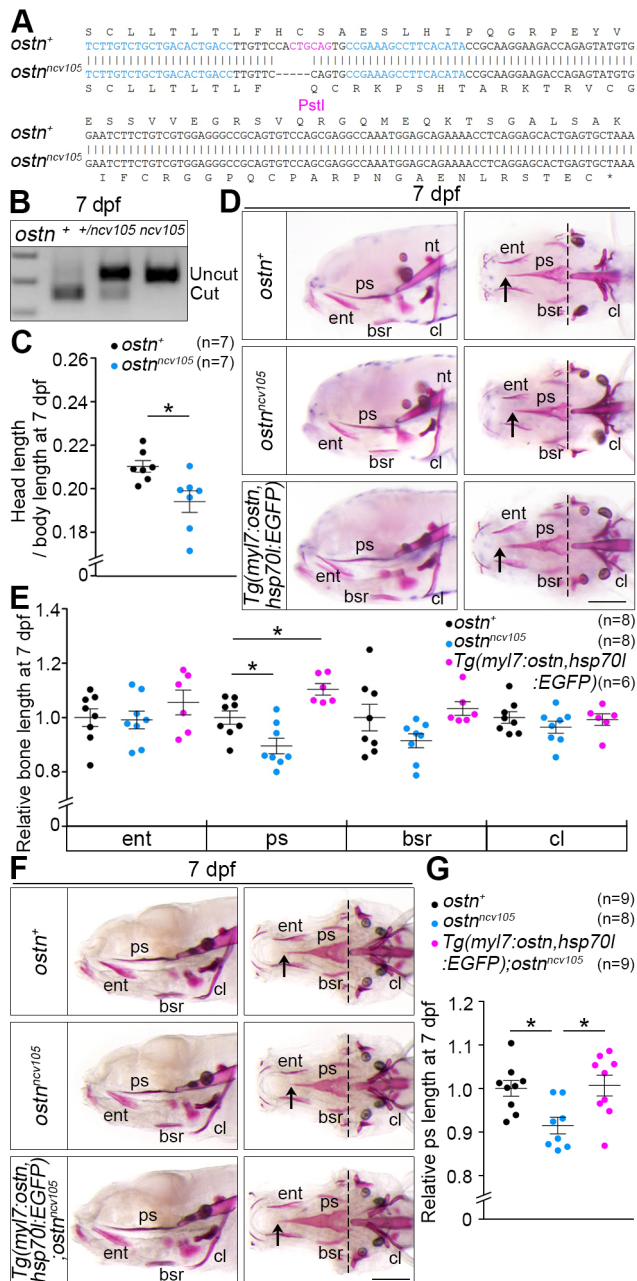

Fig. 2. Ostn is expressed in the ventricle of hearts and corpuscles of Stannius. (A) Whole-mount *in situ* hybridization (WISH) analyses of *ostn* mRNA expression in a zebrafish larva at 72 hpf (left), and *ostn* (middle) and *casr* (right) mRNA expression at corpuscles of Stannius (CS). (B) WISH analyses of *ostn* and *myl7* mRNAs of larvae at the indicated time points. Arrows indicate the ventricles. A, atrium; V, ventricle. Scale bars: 100 μm.

Fig. 3. Depletion and overexpression of Ostn result in shortening and elongation, respectively, of the parasphenoid at an early stage. (A) DNA and corresponding amino acid sequence of the *ostn^ncv105* allele. The 5 bp deletion in *ostn^ncv105* leads to the mutation of 40 amino acids followed by a premature termination (asterisk). (B) Genotype of wild-type (+), heterozygous (+/*ncv105*) and homozygous (*ncv105*) alleles as confirmed by digestion of PCR products containing a *Pst*I site as indicated in A. (C) Ratio of head length [from the tip of the upper jaw to the caudal part of the Alizarin Red stained notochord (nt)] to body length (from the tip of the upper jaw to the end of the tail) of 7 dpf wild-type (+) or homozygous mutant (*ncv105*) larvae. Each point indicates data from an individual larva. *n*, number of larvae examined. (D) Representative images of Alizarin Red staining of 7 dpf larvae of wild type (top), *ostn^ncv105* homozygous mutant (middle) and *Tg(myl7:ostn,hsp70l:EGFP)* (bottom). Lateral view (left) and ventral view (right), anterior to the left. Arrows and dashed lines indicate the tip and the top of the concave in the caudal part of the parasphenoid (ps), respectively. (E) Quantitative analyses of cranial bone length of 7 dpf *ostn^ncv105* and transgenic larvae relative to the mean length of wild-type bones is plotted for entopterygoid (ent), ps (between arrow and dashed line in D), branchiostegal ray (bsr) and cleithrum (cl). (F) Representative images of Alizarin Red staining of 7 dpf larvae of wild type (top), *ostn^ncv105* homozygous mutant (middle) and *Tg(myl7:ostn,hsp70l:EGFP);ostn^ncv105*. Views as in D. (G) Quantitative analyses of F. Data were analyzed by Student's *t*-test or one-way ANOVA with Tukey's test. **P*<0.05. Error bars indicate s.e.m. Scale bars: 200 μm.

7 dpf. Whereas the ps was shorter in *ostn^ncv105* than in wild-type larvae, other intracranial membranous bones (ent, bsr and cl) were comparable in length among *ostn^ncv105* mutants, *Tg(myl7:ostn,hsp70l:EGFP)* and wild-type larvae at 7 dpf (Fig. 3D,E). Head length of *ostn^ncv105* larvae remained shorter than in the control at 10 dpf (Fig. S4A). Consistently, the length of all the cranial bones in *ostn^ncv105* larvae was now shorter than in control larvae (Fig. S4B,C).

Next, we examined the effect of *ostn* knockdown using morpholino oligonucleotides (MOs) on the length of the ps. In *ostn* morphants, the ps was shorter than in larvae injected with vehicle (Fig. S4D-F). We confirmed that the circulation was unaffected in the *ostn* morphants (Movies 3 and 4).

To further examine the contribution of Ostn derived from CMs to bone formation, we crossed the *Tg(myl7:ostn,hsp70l:EGFP)* and *ostn^ncv105* fish. The shortened ps found in *ostn^ncv105* larvae was reversed by the overexpression of Ostn in CMs (Fig. 3F,G). These data suggest that Ostn derived from CMs might contribute to bone formation.

Ostn contributes to endochondral bone formation

We then explored the contribution of Ostn to endochondral bone formation, measuring the length of pharyngeal cartilages, ethmoid plate (ep), trabeculae (tr), Meckel's cartilage (mc), palatoquadrate (pq) and hyosymplectic (hs) in *ostn^ncv105* larvae (Schilling and Kimmel, 1997). The mc and pq were shorter in the mutant than in the control (Fig. 4A,B). In clear contrast, the ps and hs were longer in *Tg(myl7:ostn,hsp70l:EGFP)* than in the control. In addition, all except tr were longer in *Tg(myl7:ostn,hsp70l:EGFP)* than in *ostn^ncv105* larvae.

We attempted to understand the reason why these bones were shortened in the mutant larvae and elongated in larvae overexpressing Ostn. The area of the pq, in which the pterygoid process (pp) was excluded, was smaller in the mutant than in the control (Fig. 4C,D), whereas it was larger in *Tg(myl7:ostn,hsp70l:EGFP)* larvae. We then counted the number and measured the area of individual chondrocytes including extracellular matrix in the pq (Fig. 4C,E,F). Although the number of cells was comparable between mutant and control, the area of individual chondrocytes was smaller in *ostn^ncv105* larvae and greater in *Tg(myl7:ostn,hsp70l:*

deleted 5 bp. The resulting allele encoded 40 mutated amino acids from Phe18 (F), followed by a premature termination codon (Fig. 3A). We named these mutants *ostn^ncv105* and screened them by genomic PCR product digestion with *Pst*I (Fig. 3A,B). We also developed the *Tg(myl7:ostn,hsp70l:EGFP)* line, in which Ostn is expressed exclusively in the heart, to investigate the effect of overexpression of Ostn on bone formation.

Shortened heads were apparent in *ostn^ncv105* larvae (Fig. 3C, D). We further examined the length of the head and body during development from embryo and larva. Significant shortening of head length was first observed at 6 days post-fertilization (dpf), when the growth of bones and cartilage became active (Fig. S3A, B). We quantitatively measured the ratio of head length to total body length and the length of cranial bones: entopterygoid (ent), parasphenoid (ps), branchiostegal ray (bsr) and cleithrum (cl). Head length was shorter in the mutant than in the control at
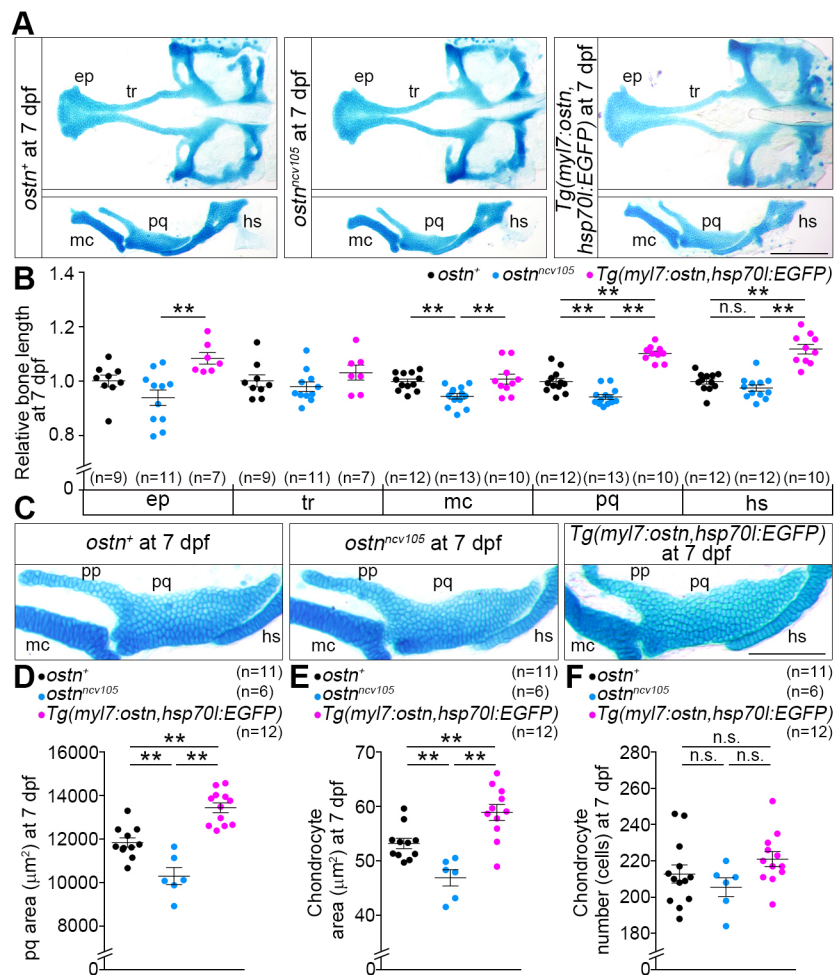
Fig. 4. Ostn regulates the growth of endochondral bone formation. (A) Representative images of Alcian Blue staining of cranial cartilages of a wild-type ($ostn^+$; left), $ostn^{ncv105}$ mutant (center) and Ostn-overexpressing [right; $Tg(myl7:ostn,hsp70l:EGFP)$] larva at 7 dpf. ep, ethmoid plate; tr, trabeculae; mc, Meckel's cartilage; pq, palatoquadrate; hs, hyosymplectic. (B) Quantitative analyses of A. Bone length relative to the mean length of wild-type bones is plotted. (C) Representative images of Alcian Blue staining of cartilages of the lower jaw of a wild-type, $ostn^{ncv105}$ mutant and Ostn-overexpressing larva at 7 dpf. pp, pterygoid process. (D) Quantitative analyses of the area of the ps of wild-type, $ostn^{ncv105}$ mutant and Ostn-overexpressing larvae at 7 dpf. (E) Quantitative analyses of the area of individual chondrocytes in the pq. (F) The number of chondrocytes in the pq. **$P<0.01$; n.s., no significant difference between two groups. Error bars indicate s.e.m. Scale bars: 200 μm in A; 100 μm in C.

$EGFP$) larvae than in the control, suggesting that Ostn might be involved in the regulation of endochondral bone formation.

Collectively, our data indicate the contribution of Ostn to both membranous and endochondral bone formation.

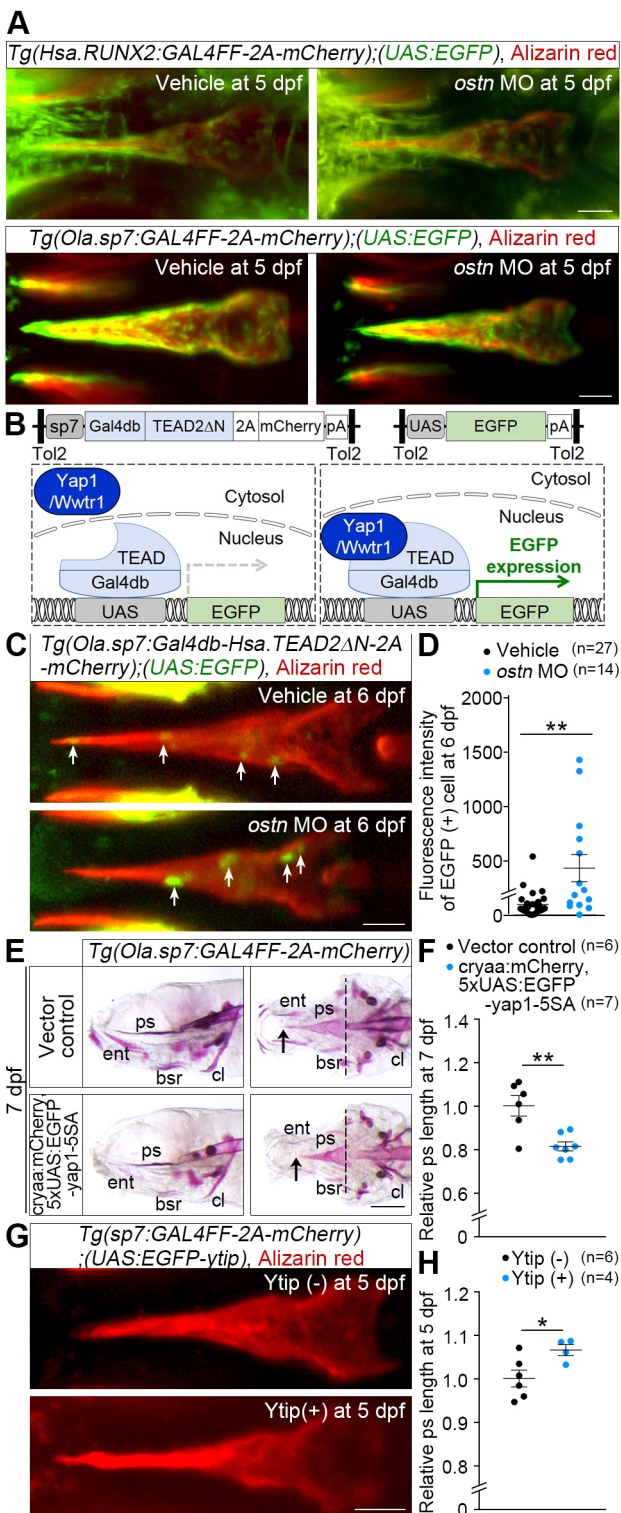## Ostn affects Yap1- or Wwtr1-dependent transcriptional regulation in the parasphenoid

The ps develops according to intramembranous ossification that requires the maturation of MSCs to osteoblasts. Runx2 is an essential transcription factor promoting the differentiation of MSCs to preosteoblasts (Komori et al., 1997; Long and Ornitz, 2013). Sp7 (osterix) is required for preosteoblast differentiation to mature osteoblasts (Zhou et al., 2010). We examined the promoter activity of these two essential transcription factors.

To observe $runx2$ promoter-dependent transcription and $sp7$ promoter-dependent transcription, respectively (Knopf et al., 2011; Spoorendonk, et al., 2008), we developed two Tg lines: $Tg(Hsa. RUNX2:GAL4FF-2A-mCherry)$ in which GAL4FF is expressed under the human (*Homo sapiens*) RUNX2 promoter; and $Tg(Ola. sp7:GAL4FF-2A-mCherry)$ in which GAL4FF is expressed under the medaka fish (*Oryzias latipes*) sp7 promoter. These Tg lines were crossed with $Tg(UAS:EGFP)$ and expression of the EGFP reporter compared with that of endogenous $runx2a/b$ and $sp7$ mRNAs (Fig. S5A,B). EGFP reporter expression in $Tg(Hsa.RUNX2: GAL4FF-2A-mCherry);(UAS:EGFP)$ or $Tg(Ola.sp7:GAL4FF-2A-mCherry);(UAS:EGFP)$ overlapped with the expression domains of endogenous $runx2a/b$ or $sp7$ mRNA as detected by WISH,

indicating that these Tg fish can be used to monitor $runx2$ and $sp7$ promoter activity. We compared EGFP fluorescence in larvae injected with vehicle with that of $ostn$ morphants. Fluorescence intensity of the ps was comparable in $ostn$ morphant and control larvae (Fig. 5A), indicating that $runx2$ and $sp7$ promoter activity is unaffected by Ostn.

The function of YAP1 and WWTR1 (TAZ) in osteogenesis has been controversial. YAP1 represses RUNX2-mediated transcription (Zaidi et al., 2004). WWTR1 functions as a coactivator for RUNX2 during MSC differentiation to osteoblast (Hong et al., 2005), while osteoblast-specific overexpression of WWTR1 enhances bone formation (Yang et al., 2013). We monitored Yap1/Wwtr1 transcriptional activity in zebrafish using $Tg(Ola.sp7:Gal4db-Hsa. TEAD2ΔN-2A-mCherry);(UAS:EGFP)$ larvae, in which nuclear translocated Yap1 or Wwtr1 induces GAL4/UAS system-driven EGFP expression (Fig. 5B). When $ostn$ was knocked down by MO, Yap1/Wwtr1-dependent transcription was increased (Fig. 5C,D), suggesting that nuclear translocation of Yap1/Wwtr1 is suppressed by Ostn-mediated signaling. Consistent with the results that there was no difference of bone length except the ps in $ostn$ mutants at 7 dpf (Fig. 3E), Yap1-dependent transcription in the op, bsr and ent at 6 dpf was comparable between $ostn$ morphants and control (Fig. S8A,B).

To test whether Yap1 regulates growth of the ps, we overexpressed the constitutively active form Yap1-5SA or the dominant-negative Yap1-Tead interfering peptide (Ytip) (von et al., 2012; Zhao et al., 2007). Larvae expressing Yap1-5SA were selected by *crystallin alpha*

Fig. 5. Ostn regulates osteogenesis through Yap1/Wwtr1. (A) *runx2* and *sp7* promoter activity monitored by EGFP in the ps of *Tg(Hsa.RUNX2: GAL4FF-2A-mCherry);(UAS:EGFP)* larvae (top) and those of *Tg(Ola.sp7: Gal4FF-2A-mCherry);(UAS:EGFP)* (bottom) treated with vehicle (left) or *ostn* MO (right). Confocal images are of larvae stained with Alizarin Red at 5 dpf. (B) Illustration of how Tg fish enable detection of nuclear translocation of Yap1/ Wwtr1 by EGFP expression in tissues where the *sp7* promoter is active. (C) Confocal images of the ps of Tg larvae injected with vehicle (top) or *ostn* MO (bottom) and stained with Alizarin Red at 6 dpf. Arrows indicate EGFP-positive cells, which correspond to those in which Yap1/Wwtr1 enter the nucleus. (D) Quantitative analysis of C. The intensity of the EGFP-positive area in the ps is plotted. The number of EGFP-positive areas quantified is indicated at the top. (E) Representative images of Alizarin Red staining of *Tg(Ola.sp7: Gal4FF-2A-mCherry)* larvae at 7 dpf transiently transfected with the plasmids indicated on the left. Lateral view (left) and ventral view (right), anterior to the left. Arrows and dashed lines indicate the tip and the top of concave of the caudal part of the ps, respectively. (F) Quantitative analyses of ps length of the larvae in E. The length of ps was measured as in Fig. 3E. (G) Representative images of Alizarin Red staining of the ps of *Tg(Ola.sp7:GAL4FF-2A-mCherry); (UAS:EGFP-ytip)* larvae at 5 dpf. (H) Quantitative analyses of G. ps length relative to the mean length of the wild-type ps was plotted. *$P<0.05$, **$P<0.01$. Error bars indicate s.e.m. Scale bars: 50 μm in A,C,G; 200 μm in E.

examined the differentiation of preosteoblasts and osteoblasts by the expression of *runx2a/b*, *sp7* and *spp1* mRNAs in *ostn^{ncv105}* mutant larvae. The expression of these genes was comparable between mutant and control larvae (Fig. S6A-D). Furthermore, we analyzed cell proliferation and apoptosis in the ps of *ostn* morphants and control. When the proliferation of ps cells marked by EGFP was analyzed by EdU incorporation, we found no difference between the two groups (Fig. S7A,C). Using another Tg fish, *Tg(Ola.sp7: EGFP)*, to directly mark cells in the ps, TUNEL staining revealed that apoptotic cells were barely or undetected in the ps of *ostn* morphant or control larvae (Fig. S7B,D). In addition, we investigated the maturation of osteoblasts and chondrocytes by the expression of *col10a1* mRNA, which is known to be inhibited by Yap1 (Deng et al., 2016). There was no significant difference in *col10a1* expression between control and *ostn^{ncv105}* larvae when examined at 4 dpf by WISH (Fig. S6E). However, when examined by quantitative (q)RT-PCR, *col10a1* mRNA expression was suppressed in *ostn^{ncv105}* larvae at 7 dpf (Fig. S6F,G).

Since *ctgfa* gene expression is promoted by Yap1 and Wwtr1 (Zhang et al., 2009; Zhao et al., 2008), we examined whether Ctgfa is involved in ps growth. When Ctgfa was overexpressed, the ps was shortened (Fig. S8C,D). By contrast, the ps of *ctgfa* morphants tended to be longer than in control morphants (Fig. S8E,F), although the difference was not significant. In addition, we confirmed the expression of *ctgfa* mRNA in the ps of control larvae (Fig. S13D), suggesting the participation of Ctgfa in ps growth. We assume that the reason why there was no significant difference in ps length between *ctgfa* morphants and control morphants is because the *ctgfa* morphants exhibiting cardia bifida, in which the expression of *ctgfa* mRNA was greatly reduced, were excluded from this analysis. These data suggest that the Yap1-Ctgfa signaling induces shortening of the ps, whereas Ostn induces elongation of the ps. These data for membranous bone growth and the data for cartilage growth suggest that Ostn contributes to growth of bones not by regulating proliferation, apoptosis or differentiation, but presumably by regulating bone matrix via a Ctgfa-dependent signal.

A (*cryaa*) promoter-driven mCherry expression in the eyes. When Yap1-5SA was transiently expressed using the *sp7* promoter and GAL4/UAS system, the ps became shortened (Fig. 5E,F). In clear contrast, when Ytip was stably expressed in the ps using the GAL4/UAS system, the ps became elongated (Fig. 5G,H). These data suggest that Ostn-dependent inhibition of a Yap1-mediated signal is involved in the growth of the membranous bones.

Yap1 is known to regulate cell proliferation, apoptosis and differentiation (Varelas, 2014; Zhao et al., 2010). Therefore, we

OSTN enhances CNP-dependent nuclear export of YAP1/WWTR1

We tried to delineate the linkage between OSTN-mediated signal and YAP1/WWTR1 using cultured osteoblasts. CNP regulates
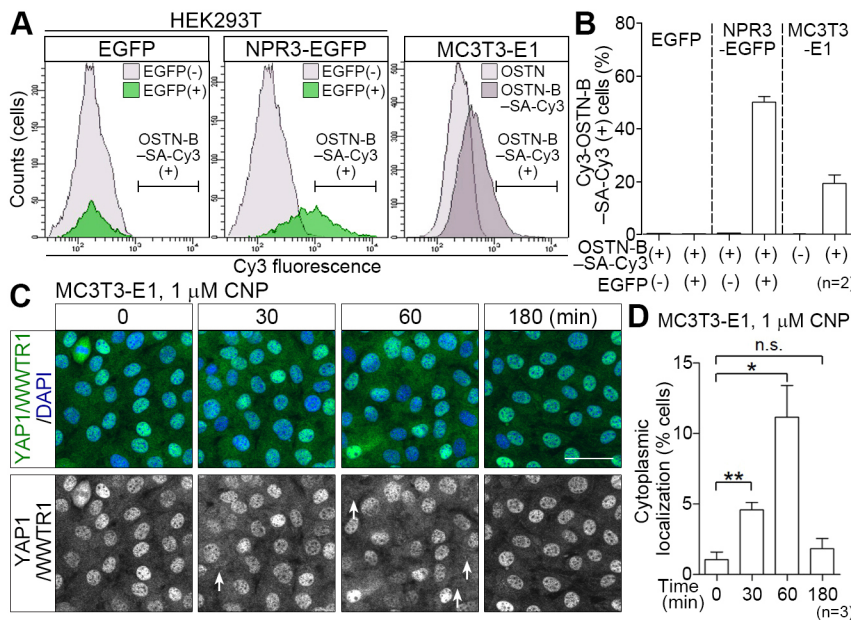
DEVELOPMENT

Fig. 6. CNP induces nuclear export of YAP1/WWTR1 in MC3T3-E1 cells. (A) Binding of biotin-labeled rat OSTN (OSTN-B) to EGFP (left) or NPR3-EGFP (center) overexpressed in HEK293T cells and that of unlabeled rat OSTN and OSTN-B to MC3T3-E1 cells (right) was analyzed by flow cytometry. Binding of OSTN-B was detected by Cy3-conjugated streptavidin (SA-Cy3). Note that OSTN-B binds to NPR3-EGFP and to endogenous receptors for OSTN expressed in MC3T3-E1 cells. (B) Quantitative analyses of A. (C) Representative images of anti-YAP1/WWTR1 immunostaining and DAPI staining of MC3T3-E1 cells stimulated with 1 μM CNP for the indicated time. Double staining with DAPI (blue) and YAP1/ WWTR1 (green) (top) and YAP1/WWTR1 staining alone (bottom) are shown. Arrows indicate cells exhibiting nuclear export of YAP1/WWTR1. (D) Quantitative analyses of nuclear export of YAP1/WWTR1 in C using three sets of cells. In each set, more than 100 cells were analyzed for immunoreactivity of YAP1/WWTR1. *$P<0.05$, **$P<0.01$; n.s., no significant difference between two groups. Error bars indicate s.e.m. Scale bar: 50 μm.

osteoblast differentiation through NPR2 (Suda et al., 1996). We assumed that OSTN might modify CNP-dependent signaling in osteoblasts, as OSTN is reported to bind to NPR3 to block binding of NPs to NPR3 (Moffatt et al., 2007). We first confirmed that OSTN binds to C-terminally EGFP-tagged NPR3 (NPR3-EGFP) in cultured cells using flow cytometry. HEK293T cells expressing NPR3-EGFP were bound to biotin-labeled rat (*Rattus norvegicus*) OSTN, which was detected by Cy3-conjugated streptavidin (Fig. 6A,B, Fig. S9A,C). Osteoblastic MC3T3-E1 cells also bound to OSTN (Fig. 6A,B). The binding of OSTN to NPR3-EGFP was competitive with CNP (Fig. S9B,C).

We further examined how CNP and OSTN affect the localization of YAP1 and WWTR1 in MC3T3-E1 cells. CNP induced nuclear export of YAP1/WWTR1 in a time-dependent (Fig. 6C,D) and dose-dependent (Fig. 7A,B) manner. This dose-dependent nuclear export paralleled an increase in cGMP (Fig. 7C) and reached a plateau when the cells were stimulated with 1 μM CNP. Even when induced with this saturated dose of CNP (1 μM), the nuclear export of YAP1/WWTR1 was enhanced by OSTN, whereas 1 μM OSTN alone did not induce nuclear export (Fig. 7D,E). CNP- and CNP/OSTN-dependent nuclear export of YAP1/WWTR1 was completely inhibited by the protein kinase G (PKG) inhibitor KT5823 (Fig. 7D,E), suggesting that cGMP-PKG signaling, presumably through CNP-activated NPR2, is essential for determining the localization of YAP1/WWTR1.

The consequence of nuclear export of YAP1/WWTR1 was reflected in the reduction of *Ctgf* mRNA expression when the cells were stimulated with CNP. A greater reduction in *Ctgf* mRNA was observed in cells stimulated with both 1 μM CNP and 1 μM OSTN, but not in those pretreated with KT5823 (Fig. 7F). Notably, MC3T3-E1 cells treated with 1 μM CNP still bound to 0.1 μM OSTN (Fig. 7G,H). The amount of biotin-labeled rat OSTN (0.1 μM) that bound to NPR3 was decreased by either unlabeled rat OSTN or CNP (Fig. S9A-C). Cy3-conjugated streptavidin was detected in MC3T3-E1 cells that were neither treated with unlabeled rat OSTN nor with biotin alone. Biotin-labeled rat OSTN (0.1 μM) binding to MC3T3-E1 cells was not affected by insulin, which was used as a negative control (Fig. S10A,B). Collectively, these data suggest that OSTN can bind to unidentified receptors besides NPR3 in MC3T3-E1 cells.

Because we found that endochondral bone formation was regulated by Ostn in zebrafish (Fig. 4), we examined the effect of Ostn on CNP-dependent localization of YAP1/WWTR1 in mouse chondrogenic ATDC5 cells. CNP induced nuclear export of YAP1/WWTR1 in both a time- and dose-dependent manner in ATDC5 cells, similar to MC3T3-E1 cells (Fig. S11A-D). These data indicate that a CNP-dependent signal induces the nuclear export of YAP1/WWTR1 in chondrogenic cells.

Enhancement of CNP-regulated nuclear export of YAP1/WWTR1 by OSTN depends on an NPR2-PKG signaling axis

We then examined whether CNP-induced nuclear export of YAP1/WWTR1 depends on NPR2. qRT-PCR analyses of *Npr2* mRNA in MC3T3-E1 cells treated with siRNA revealed the effective knockdown of *Npr2* (Fig. 8A, Fig. S12A). Furthermore, CNP-induced cGMP production, presumably through NPR2, was abolished in *Npr2* knockdown cells (Fig. 8B, Fig. S12B). Thus, we tested the effect of a reduction of *Npr2* on CNP-dependent nuclear export of YAP1/WWTR1 in the cells treated with these siRNAs. Nuclear export of YAP1/WWTR1 was reduced in the *Npr2* knockdown cells (Fig. 8C,D, Fig. S12C,D). Collectively, in osteoblasts, activation of NPR2 by CNP followed by PKG activation results in nuclear export of YAP1/WWTR1.

An increase in Yap1/Wwtr1-dependent transcription, as revealed by the EGFP reporter, in the ps of *ostn* morphants reflected the nuclear localization of Yap1/Wwtr1 (Fig. 5C), suggesting that a similar Npr2-mediated signal is activated in ps formation. The ps was shortened when Yap1/Wwtr1 were localized in nuclei, suggesting that activation of Yap1/Wwtr1 transcription results in shortening of the ps. To test whether an Npr2-dependent signal participates in ps formation, we examined how the reduction of Npr2 expression affects ps formation. Beforehand, we analyzed the expression of *npr2*, *npr3* and *nppcl* (*wu:fj39g12*) mRNAs. WISH analyses revealed that *npr2* mRNA is detected in head mesenchyme, pectoral fin bud/pectoral fin, ceratohyal and hyosymplectic. *npr3* mRNA was detected in the midbrain-hindbrain boundary and floor plate. *nppcl* mRNA was also detected in the brain (Fig. S13A-C). The *npr2* and *npr3* mRNAs were barely detected in the ps of larvae at 5 dpf (Fig. S13D). These
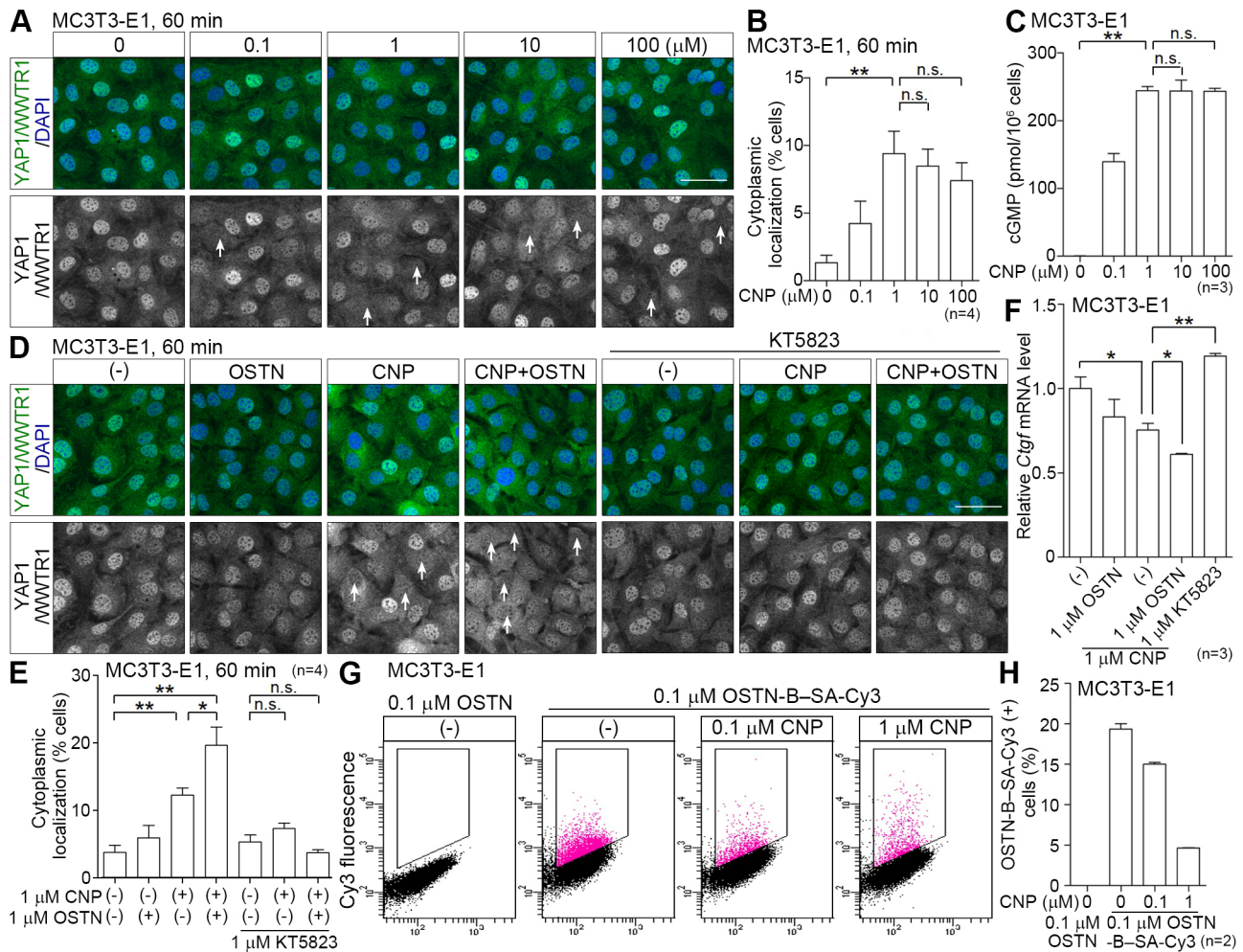
Fig. 7. OSTN enhances CNP-induced nuclear export of YAP1/WWTR1 in MC3T3-E1 cells. (A) Representative images of anti-YAP1/WWTR1 immunostaining and DAPI staining of MC3T3-E1 cells stimulated for 60 min with CNP at the doses indicated. (B) Quantitative analyses of nuclear export of YAP1/WWTR1 in A using four sets of cells. In each set, more than 100 cells were analyzed for immunoreactivity of YAP1/WWTR1. (C) Measurement of cGMP in MC3T3-E1 cells stimulated with CNP at the doses indicated for 15 min. (D) Representative images of anti-YAP1/WWTR1 immunostaining and DAPI staining of MC3T3-E1 cells pretreated with or without the PKG inhibitor KT5823 (1 µM) and stimulated for 60 min with CNP (1 µM) and Ostn (1 µM) as indicated on the top. Arrows indicate cells exhibiting cytoplasmic localization of YAP1/WWTR1. (E) The nuclear export of YAP1/WWTR1 in cells under the condition described in D were analyzed similar to B. (F) *Ctgf* mRNA expression analyzed by qRT-PCR using mRNAs obtained from MC3T3-E1 cells stimulated with the peptides and treated with KT5823 as indicated for 120 min. (G) Competitive binding of OSTN with CNP to MC3T3-E1 cells was analyzed by flow cytometry. The binding of OSTN-B in the presence of CNP to MC3T3-E1 cells is shown in the form of dot plot data. (H) Quantitative analyses of G. *$P<0.05$, **$P<0.01$; n.s., no significant difference between two groups. Error bars indicate s.e.m. Scale bars: 50 µm.

data suggest that at least Nppcl-Npr2/Npr3 might function in zebrafish, although we failed to detect their expression in the ps.

The MOs against *npr2* were validated by examining splicing efficiency (Fig. S14A). *npr2* morphants exhibited a shortened ps at 5 dpf (Fig. 8E,F). Furthermore, this shortening of the ps was rescued by the injection of *npr2* mRNA into the larvae at 7 dpf (Fig. S14B,C). These data indicate that an Npr2-mediated signal is involved in the regulation of bone growth *in vivo*.

DISCUSSION

We identified Ostn as an endocrine hormone produced in the heart that regulates osteogenesis and chondrogenesis in zebrafish. Besides ANP and BNP, no endocrine hormones affecting remote organs have been reported for the heart. Although OSTN is proposed to belong to the NP family, it lacks the cysteine residues that render itself circular via a disulfide bridge that is conserved among the NP family members ANP, BNP and CNP (Potter et al., 2006; Riley and Smart,

2011). In addition, OSTN binds to NPR3 but not NPR2, thereby augmenting CNP-dependent NPR2 activation by inhibiting clearance of CNP in chondrocytes but not in osteoblasts (Moffatt et al., 2007). In agreement with this notion, our data suggest that Ostn contributes to both membranous bone formation and endochondral bone formation by inducing nuclear export of Yap1/Wwtr1. The present data also suggest that Ostn activates an unidentified receptor to regulate osteogenesis in zebrafish. Therefore, we provide evidence that the heart secretes a novel peptide regulating bone formation, although it is unlikely to belong to the NP family.

We found that membranous bones and endochondral bones were shortened in *ostn*[ncv105] mutant larvae. At the early stage, Ostn specifically affected the growth of the ps among the cranial bones that develop according to intramembranous ossification. The ps develops earlier than other bones (Verreijdt et al., 2006) and so we could detect its shortening at an early stage (7 dpf). At the later stage, the other membranous bones were also shortened. Furthermore, cartilages were
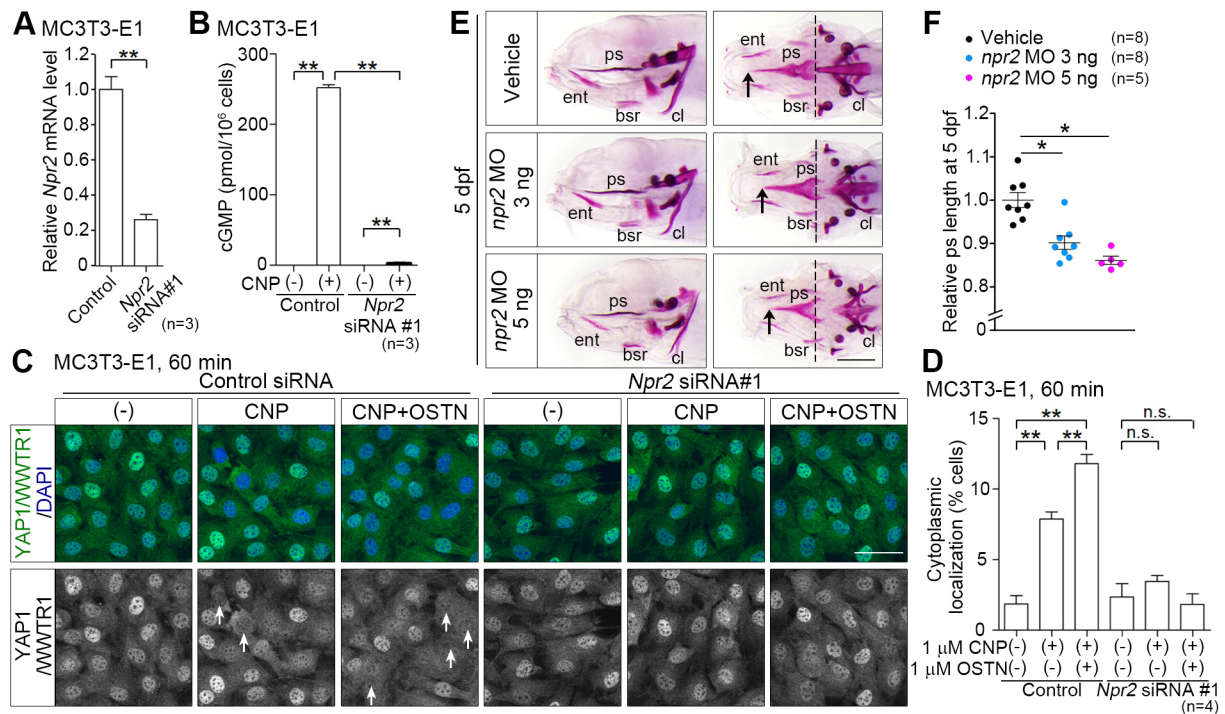
Fig. 8. CNP-induced nuclear export of YAP1/WWTR1 depends on NPR2. (A) qRT-PCR analyses validate the knockdown efficiency of siRNAs directed against *Npr2* mRNAs. MC3T3-E1 cells were treated with *Npr2* siRNA for 72 h. (B) cGMP levels in MC3T3-E1 cells pretreated with siRNAs for 72 h and stimulated with 1 μM CNP for 15 min as indicated. (C) Representative images of anti-YAP1/WWTR1 immunostaining and DAPI staining of MC3T3-E1 cells pretreated with either control siRNA or *Npr2* siRNA#1 and simulated with peptide (1 μM CNP and/or 1 μM OSTN) as indicated. Arrows indicate cells exhibiting nuclear export of YAP1 and WWTR1. (D) The nuclear export of YAP1/WWTR1 in the cells in C was analyzed similar to in Fig. 6D. (E) Representative images of Alizarin Red staining of 5 dpf larvae injected with vehicle, 3 ng or 5 ng *npr2* MO. Arrows and dashed lines indicate the tip and top of concave of the caudal end of the ps, respectively. (F) The length of ps in E was measured similar to in Fig. 3E. *P<0.05, **P<0.01; n.s., no significant difference between two groups. Error bars indicate s.e.m. Scale bars: 50 μm in C; 200 μm in E.

shortened. These data suggest that a common signaling pathway regulates the growth of both bone types. Mammalian chondrocytes express *Runx2* and *Col10a1*, and zebrafish osteoblasts express these genes (Li et al., 2009). We noted no alteration of *runx2* expression in *ostn*[ncv105] larvae. Therefore, an Ostn-mediated signal might be involved in promoting the expression of genes essential for bone matrix apposition.

OSTN augments the CNP-dependent nuclear export of YAP1/ WWTR1 in osteoblasts and chondrocytes. It is of note that CNP induces the export of YAP1/WWTR1 in these cells. There have been no reports that NPs regulate the localization of YAP1/WWTR1. Inhibition of PKG inhibited the export of YAP1/WWTR1. Although protein kinase A, another Ser/Thr kinase, is reported to determine the localization of YAP1 through LATS kinase (Iglesias-Bartolome et al., 2015; Kim et al., 2013), PKG-dependent regulation has not been reported. *Ostn* Tg mice exhibit elongated bones and kyphosis, which are also found in *Bnp* Tg, *Cnp* Tg and *Npr3* knockout mice (Jaubert et al., 1999; Kake et al., 2009; Matsukawa et al., 1999; Yasoda et al., 2004). Elongation of bones is ascribed to modulation of CNP-NPR3 signaling by OSTN in chondrocytes (Moffatt et al., 2007). OSTN binds to NPR3 and is proposed to inhibit clearance of CNP, resulting in augmentation of a CNP-dependent signal. Notably, OSTN augmented YAP1/WWTR1 nuclear export at a saturating concentration of CNP for NP receptors. These results suggested that OSTN binds to an unidentified receptor to modulate CNP-dependent signaling downstream of NPR2, as OSTN itself did not induce nuclear export of YAP1/WWTR1 in osteoblasts. We need to identify the OSTN-specific receptor in order to clearly delineate the OSTN signaling that is not through NPR3.

The role for a YAP1/WWTR1-dependent signal in osteogenesis remains controversial. WWTR1 regulates the differentiation of MSCs to osteoblasts (Hong et al., 2005). On the one hand, overexpression of WWTR1 in mice leads to an increased bone mass via RUNX2-dependent transcription (Yang et al., 2013). On the other hand, YAP1 binds to RUNX2 to represses its transcriptional activity (Zaidi et al., 2004). One group reports that fibroblast growth factor 2 (FGF2) downregulates WWTR1 in MC3T3-E1 cells to induce their proliferation (Eda et al., 2008), whereas another group demonstrated that FGF2 induces the differentiation of osteoblasts (Byun et al., 2014). Therefore, it is still controversial how YAP1/ WWTR1 function in osteoblasts after their differentiation from MSCs *in vivo*. Proliferation, differentiation and apoptosis of osteoblasts are not altered in *ostn* morphants. However, chondrocytes were smaller in *ostn* mutants than in the control, suggesting that a Yap1/Wwtr1-mediated signal might participate in bone matrix deposition or mineralization. Expression of *col10a1* mRNA was decreased in *ostn*[ncv105] larvae at 7 dpf. Because mRNAs were prepared from whole larvae, it is unclear whether this decrease was attributable to that in osteoblasts or chondrocytes. Expression of Col10a1 has been reported to be transcriptionally inhibited by Yap1 (Deng et al., 2016), and our results are consistent with this.

CTGF-dependent bone formation appears to be complicated. While *Ctgf*-deficient mice show impaired chondrocyte proliferation and matrix composition in the hypertrophic chondrocytes (Ivkovic et al., 2003), overexpression of CTGF from the osteocalcin promoter results in impairment of osteoblast activity due to decreased mineral apposition (Smerdel-Ramoya et al., 2008). However, another study reports that CTGF-deficient osteoblasts
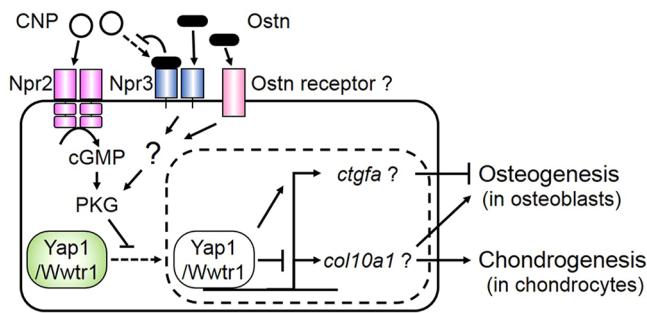
Fig. 9. Model for how Ostn regulates bone formation. (A) In zebrafish osteoblasts and chondrocytes, CNP induces nuclear export of Yap1/Wwtr1 through Npr2-cGMP-PKG signaling. Because Yap1 is known to inhibit the transcription of *col10a1*, Ostn might induce nuclear export of Yap1 and the subsequent expression of Col10a1 in osteoblasts and chondrocytes and subsequent repression of Ctgfa in osteoblasts. Collectively, Ostn secreted from the heart and other tissues binds to Npr3 and the unidentified Ostn receptor to enhance the CNP-induced nuclear export of Yap1/Wwtr1 and promote osteogenesis and chondrogenesis.

exhibit reduced proliferation but normal mineralization (Mundy et al., 2014). These results suggest that CTGF expression promoted by YAP1/WWTR1 might function in bone formation in a stage-dependent and cell-dependent manner.

Ostn from the CS, which controls calcium homeostasis, might also contribute to bone formation. We found that Ostn is expressed in the CS where Casr and stanniocalcin are expressed (Lin et al., 2014; Tseng et al., 2009). In the CS, Casr senses the extracellular Ca^{2+} and regulates stanniocalcin, which acts on Na^+/K^+-ATPase-rich cells in zebrafish that function in Ca^{2+} absorption (Tseng et al., 2009). Therefore, if Ostn regulates Ca^{2+} balance through the CS, the impaired bone formation found in *ostn^{ncv105}* larvae might be ascribed to dysfunction of the CS.

In summary, we demonstrate that Ostn produced in CMs contributes to the formation of both membranous and endochondral bone (Fig. 9). OSTN enhanced peak CNP-dependent nuclear export of YAP1/WWTR1 in osteoblasts and chondrocytes. Our data suggest that Ostn regulates osteogenesis and chondrogenesis in zebrafish cooperatively through NP-dependent signaling and through an unidentified Ostn receptor-mediated signaling.

MATERIALS AND METHODS
Zebrafish husbandry
Zebrafish were maintained under standard conditions (Westerfield, 2007). Experiments using zebrafish were approved by the Institutional Animal Committee of the National Cerebral and Cardiovascular Center and performed according to the guidelines of the institute. Embryos and larvae were staged by hpf at 28°C (Kimmel et al., 1995).

Plasmids
Construction of Tol2-based plasmids used to establish Tg zebrafish lines is described in the supplementary Materials and Methods. Primers for cloning are listed in Table S1.

Tg and mutant fish lines
Transgenic zebrafish lines and the *ostn^{ncv105}* mutant line were established as described in the supplementary Materials and Methods. The *Tg(UAS:EGFP)* fish line was provided by K. Kawakami (National Institute of Genetics, Japan; Asakawa et al., 2008). Primers for genotyping are listed in Table S1.

FACS and RNA-seq
mCherry-positive or tdEos-positive cells were isolated by FACS (see the supplementary Materials and Methods) from *Tg(myl7:NLS-mCherry)* or

Tg(myl7:actn2-tdEos) larvae, respectively. The isolated cells were subjected to RNA-seq analyses as described in the supplementary Materials and Methods.

RT-PCR
Total RNA was isolated from zebrafish larvae, mouse organs or mouse MC3T3-E1 cells for RT-PCR of cDNA as described in the supplementary Materials and Methods. RT-PCR primers are listed in Table S1.

WISH
Zebrafish embryos and larvae at 1-4 dpf were hybridized with digoxigenin-labeled antisense RNA probes as described in the supplementary Materials and Methods.

Bone staining
Zebrafish larvae at 5-10 dpf were stained for membranous bones with Alizarin Red S and for cartilage with Alcian Blue 8GX as described in the supplementary Materials and Methods.

Microinjection of MOs and mRNA
For gene knockdown, one-cell stage zebrafish embryos were injected with *ostn*, *npr2*, *ctgfa* or control MOs. For protein overexpression, mRNA was injected into one-cell stage zebrafish embryos. For details see the supplementary Materials and Methods.

Cell culture and siRNA-mediated knockdown
Mouse MC3T3-E1, ATDC5 and human HEK293T cells were cultured, and transfections with plasmids or siRNAs (Table S2) were performed, as described in the supplementary Materials and Methods.

Microscopy, image processing and movies
Larvae were anesthetized and mounted in 1% low-melting agarose on a 35 mm diameter glass-base dish (Asahi Techno Glass) as previously described (Kashiwada et al., 2015). Fluorescence images were recorded with a FV1000 or FV1200 confocal microscope with 20× water objective lens (XLUMPlanFL, 1.0 NA) or a FV1000PME multi-photon microscope with 25× water objective lens (XLPlan, 1.05 NA) (all Olympus). Images were processed with FV10-ASW 4.1 software (Olympus) and analyzed using Imaris 7.7.1 software (Bitplane). Head length was measured using a stereo microscope as described in the supplementary Materials and Methods. Larval heart beat was recorded by lightsheet microscopy or in brightfield movies as described in the supplementary Materials and Methods.

OSTN binding assay
Streptavidin-conjugated Cy3 was incubated with biotin-labeled rat OSTN to form OSTN-B–SA-Cy3. HEK293T cells expressing NPR3-EGFP or EGFP and MC3T3-E1 cells were suspended, incubated with OSTN-B–SA-Cy3, and fluorescence intensities measured by FACS as described in the supplementary Materials and Methods.

Apoptosis and cell proliferation assays
Apoptotic cells in 6 dpf zebrafish larvae were assessed by TUNEL assay, and the proliferation of cells in 5 dpf zebrafish larvae was analyzed by EdU incorporation, as described in the supplementary Materials and Methods.

cGMP
cGMP was measured in MC3T3-E1 cells stimulated with CNP as described in the supplementary Materials and Methods.

Immunocytochemical analyses
MC3T3-E1 and ATDC5 cells were subjected to immunocytochemistry with anti-YAP1/WWTR1 antibody (Santa Cruz, sc-101199) at 1:300 as described in the supplementary Materials and Methods.

DEVELOPMENT

Quantitative analyses of fluorescence

To quantify Yap1/Wwtr1 transcriptional activity in zebrafish membranous bone, confocal stack fluorescence images of EGFP and Alizarin Red in the membranous bone regions of *Tg(Ola.sp7:Gal4db-Hsa.TEAD2ΔN-2A-mCherry);(UAS:EGFP)* 6 dpf larvae were recorded. The mean EGFP fluorescence intensity within a 100 μm^2 circle of EGFP-positive cells was measured using the FV10-ASW 4.1 software.

To quantify the percentage of MC3T3-E1 and ATDC5 cells showing YAP1/WWTR1 cytoplasmic localization, the mean fluorescence intensity of YAP1/WWTR1 staining inside a circle (8 μm in diameter) in the cytoplasm or nucleus was measured for each cell using MetaMorph software (Molecular Devices). Cells with a ratio of cytoplasmic to nuclear intensity of greater than one were considered to be positive for the cytoplasmic localization of YAP1/WWTR1. The percentage of cells showing cytoplasmic localization among total cells was calculated using unbiased images of four different microscopy fields.

Statistical analysis

Data are represented as mean±s.e.m. Statistical significance was determined by Student's *t*-test for paired samples or by one-way analysis of variance (ANOVA) with Turkey's test. $P<0.05$ was considered statistically significant.

References

Arita, Y., Nakaoka, Y., Matsunaga, T., Kidoya, H., Yamamizu, K., Arima, Y., Kataoka-Hashimoto, T., Ikeoka, K., Yasui, T., Masaki, T. et al. (2014). Myocardium-derived angiopoietin-1 is essential for coronary vein formation in the developing heart. *Nat. Commun.* **5**, 4552.

Asakawa, K., Suster, M. L., Mizusawa, K., Nagayoshi, S., Kotani, T., Urasaki, A., Kishimoto, Y., Hibi, M. and Kawakami, K. (2008). Genetic dissection of neural circuits by Tol2 transposon-mediated Gal4 gene and enhancer trapping in zebrafish. *Proc. Natl. Acad. Sci. USA* **105**, 1255-1260.

Becker, J. R., Chatterjee, S., Robinson, T. Y., Bennett, J. S., Panakova, D., Galindo, C. L., Zhong, L., Shin, J. T., Coy, S. M., Kelly, A. E. et al. (2014). Differential activation of natriuretic peptide receptors modulates cardiomyocyte proliferation during development. *Development* **141**, 335-345.

Byun, M. R., Kim, A. R., Hwang, J.-H., Kim, K. M., Hwang, E. S. and Hong, J.-H. (2014). FGF2 stimulates osteogenic differentiation through ERK induced TAZ expression. *Bone* **58**, 72-80.

Dauphinee, S. M., Eva, M. M., Yuki, K. E., Herman, M., Vidal, S. M. and Malo, D. (2013). Characterization of two ENU-induced mutations affecting mouse skeletal morphology. *G3 (Bethesda)* **3**, 1753-1758.

Deng, Y., Wu, A., Li, P., Li, G., Qin, L., Song, H. and Mak, K. K. (2016). Yap1 regulates multiple steps of chondrocyte differentiation during skeletal development and bone repair. *Cell Rep.* **14**, 2224-2237.

Eda, H., Aoki, K., Marumo, K., Fujii, K. and Ohkawa, K. (2008). FGF-2 signaling induces downregulation of TAZ protein in osteoblastic MC3T3-E1 cells. *Biochem. Biophys. Res. Commun.* **366**, 471-475.

Hagiwara, H., Sakaguchi, H., Itakura, M., Yoshimoto, T., Furuya, M., Tanaka, S. and Hirose, S. (1994). Autocrine regulation of rat chondrocyte proliferation by natriuretic peptide C and its receptor, natriuretic peptide receptor-B. *J. Biol. Chem.* **269**, 10729-10733.

Hong, J.-H., Hwang, E. S., McManus, M. T., Amsterdam, A., Tian, Y., Kalmukova, R., Mueller, E., Benjamin, T., Spiegelman, B. M., Sharp, P. A. et al. (2005). TAZ, a transcriptional modulator of mesenchymal stem cell differentiation. *Science* **309**, 1074-1078.

Iglesias-Bartolome, R., Torres, D., Marone, R., Feng, X., Martin, D., Simaan, M., Chen, M., Weinstein, L. S., Taylor, S. S., Molinolo, A. A. et al. (2015). Inactivation of a Galpha(s)-PKA tumour suppressor pathway in skin stem cells initiates basal-cell carcinogenesis. *Nat. Cell Biol.* **17**, 793-803.

Ivkovic, S., Yoon, B. S., Popoff, S. N., Safadi, F. F., Libuda, D. E., Stephenson, R. C., Daluiski, A. and Lyons, K. M. (2003). Connective tissue growth factor coordinates chondrogenesis and angiogenesis during skeletal development. *Development* **130**, 2779-2791.

Jaubert, J., Jaubert, F., Martin, N., Washburn, L. L., Lee, B. K., Eicher, E. M. and Guenet, J.-L. (1999). Three new allelic mouse mutations that cause skeletal overgrowth involve the natriuretic peptide receptor C gene (Npr3). *Proc. Natl. Acad. Sci. USA* **96**, 10278-10283.

Kake, T., Kitamura, H., Adachi, Y., Yoshioka, T., Watanabe, T., Matsushita, H., Fujii, T., Kondo, E., Tachibe, T., Kawase, Y. et al. (2009). Chronically elevated plasma C-type natriuretic peptide level stimulates skeletal growth in transgenic mice. *Am. J. Physiol. Endocrinol. Metab.* **297**, E1339-E1348.

Karsenty, G., Kronenberg, H. M. and Settembre, C. (2009). Genetic control of bone formation. *Annu. Rev. Cell Dev. Biol.* **25**, 629-648.

Kashiwada, T., Fukuhara, S., Terai, K., Tanaka, T., Wakayama, Y., Ando, K., Nakajima, H., Fukui, H., Yuge, S., Saito, Y. et al. (2015). beta-Catenin-dependent transcription is central to Bmp-mediated formation of venous vessels. *Development* **142**, 497-509.

Kim, M., Kim, M., Lee, S., Kuninaka, S., Saya, H., Lee, H., Lee, S. and Lim, D.-S. (2013). cAMP/PKA signalling reinforces the LATS-YAP pathway to fully suppress YAP in response to actin cytoskeletal changes. *EMBO J.* **32**, 1543-1555.

Kimmel, C. B., Ballard, W. W., Kimmel, S. R., Ullmann, B. and Schilling, T. F. (1995). Stages of embryonic development of the zebrafish. *Dev. Dyn.* **203**, 253-310.

Knopf, F., Hammond, C., Chekuru, A., Kurth, T., Hans, S., Weber, C. W., Mahatma, G., Fisher, S., Brand, M., Schulte-Merker, S. et al. (2011). Bone regenerates via dedifferentiation of osteoblasts in the zebrafish fin. *Dev. Cell* **20**, 713-724.

Komatsu, Y., Chusho, H., Tamura, N., Yasoda, A., Miyazawa, T., Suda, M., Miura, M., Ogawa, Y. and Nakao, K. (2002). Significance of C-type natriuretic peptide (CNP) in endochondral ossification: analysis of CNP knockout mice. *J. Bone Miner. Metab.* **20**, 331-336.

Komori, T., Yagi, H., Nomura, S., Yamaguchi, A., Sasaki, K., Deguchi, K., Shimizu, Y., Bronson, R. T., Gao, Y.-H., Inada, M. et al. (1997). Targeted disruption of Cbfa1 results in a complete lack of bone formation owing to maturational arrest of osteoblasts. *Cell* **89**, 755-764.

Li, N., Felber, K., Elks, P., Croucher, P. and Roehl, H. H. (2009). Tracking gene expression during zebrafish osteoblast differentiation. *Dev. Dyn.* **238**, 459-466.

Lin, C.-H., Su, C.-H. and Hwang, P.-P. (2014). Calcium-sensing receptor mediates Ca(2+) homeostasis by modulating expression of PTH and stanniocalcin. *Endocrinology* **155**, 56-67.

Long, F. and Ornitz, D. M. (2013). Development of the endochondral skeleton. *Cold Spring Harb. Perspect. Biol.* **5**, a008334.

Matsukawa, N., Grzesik, W. J., Takahashi, N., Pandey, K. N., Pang, S., Yamauchi, M. and Smithies, O. (1999). The natriuretic peptide clearance receptor locally modulates the physiological effects of the natriuretic peptide system. *Proc. Natl. Acad. Sci. USA* **96**, 7403-7408.

Moffatt, P. and Thomas, G. P. (2009). Osteocrin–beyond just another bone protein? *Cell Mol. Life Sci.* **66**, 1135-1139.

Moffatt, P., Thomas, G., Sellin, K., Bessette, M.-C., Lafreniere, F., Akhouayri, O., St-Arnaud, R. and Lanctot, C. (2007). Osteocrin is a specific ligand of the natriuretic Peptide clearance receptor that modulates bone growth. *J. Biol. Chem.* **282**, 36454-36462.

Mundy, C., Gannon, M. and Popoff, S. N. (2014). Connective tissue growth factor (CTGF/CCN2) negatively regulates BMP-2 induced osteoblast differentiation and signaling. *J. Cell Physiol.* **229**, 672-681.

Nishizawa, H., Matsuda, M., Yamada, Y., Kawai, K., Suzuki, E., Makishima, M., Kitamura, T. and Shimomura, I. (2004). Musclin, a novel skeletal muscle-derived secretory factor. *J. Biol. Chem.* **279**, 19391-19395.

DEVELOPMENT

Ogawa, T. and de Bold, A. J. (2014). The heart as an endocrine organ. *Endocr. Connect.* **3**, R31-R44.

Potter, L. R., Abbey-Hosch, S. and Dickey, D. M. (2006). Natriuretic peptides, their receptors, and cyclic guanosine monophosphate-dependent signaling functions. *Endocr. Rev.* **27**, 47-72.

Riley, P. R. and Smart, N. (2011). Vascularizing the heart. *Cardiovasc. Res.* **91**, 260-268.

Schilling, T. F. and Kimmel, C. B. (1997). Musculoskeletal patterning in the pharyngeal segments of the zebrafish embryo. *Development* **124**, 2945-2960.

Smerdel-Ramoya, A., Zanotti, S., Stadmeyer, L., Durant, D. and Canalis, E. (2008). Skeletal overexpression of connective tissue growth factor impairs bone formation and causes osteopenia. *Endocrinology* **149**, 4374-4381.

Soltanoff, C. S., Yang, S., Chen, W. and Li, Y.-P. (2009). Signaling networks that control the lineage commitment and differentiation of bone cells. *Crit. Rev. Eukaryot. Gene Expr.* **19**, 1-46.

Spoorendonk, K. M., Peterson-Maduro, J., Renn, J., Trowe, T., Kranenbarg, S., Winkler, C. and Schulte-Merker, S. (2008). Retinoic acid and Cyp26b1 are critical regulators of osteogenesis in the axial skeleton. *Development* **135**, 3765-3774.

Stepan, H., Leitner, E., Siems, W.-E., Maul, B. and Walther, T. (1999). mRNA quantification of C-type natriuretic peptide in brain areas of rodents. *Peptides* **20**, 1243-1245.

Stepan, H., Faber, R., Stegemann, S., Schultheiss, H.-P. and Walther, T. (2002). Expression of C-type natriuretic peptide in human placenta and myometrium in normal pregnancies and pregnancies complicated by intrauterine growth retardation. Preliminary results. *Fetal Diagn. Ther.* **17**, 37-41.

Subbotina, E., Sierra, A., Zhu, Z., Gao, Z., Koganti, S. R. K., Reyes, S., Stepniak, E., Walsh, S. A., Acevedo, M. R., Perez-Terzic, C. M. et al. (2015). Musclin is an activity-stimulated myokine that enhances physical endurance. *Proc. Natl. Acad. Sci. USA* **112**, 16042-16047.

Suda, M., Tanaka, K., Fukushima, M., Natsui, K., Yasoda, A., Komatsu, Y., Ogawa, Y., Itoh, H. and Nakao, K. (1996). C-type natriuretic peptide as an autocrine/paracrine regulator of osteoblast. Evidence for possible presence of bone natriuretic peptide system. *Biochem. Biophys. Res. Commun.* **223**, 1-6.

Suda, M., Ogawa, Y., Tanaka, K., Tamura, N., Yasoda, A., Takigawa, T., Uehira, M., Nishimoto, H., Itoh, H., Saito, Y. et al. (1998). Skeletal overgrowth in transgenic mice that overexpress brain natriuretic peptide. *Proc. Natl. Acad. Sci. USA* **95**, 2337-2342.

Tamura, N., Doolittle, L. K., Hammer, R. E., Shelton, J. M., Richardson, J. A. and Garbers, D. L. (2004). Critical roles of the guanylyl cyclase B receptor in endochondral ossification and development of female reproductive organs. *Proc. Natl. Acad. Sci. USA* **101**, 17300-17305.

Thomas, G., Moffatt, P., Salois, P., Gaumond, M.-H., Gingras, R., Godin, E., Miao, D., Goltzman, D. and Lanctot, C. (2003). Osteocrin, a novel bone-specific secreted protein that modulates the osteoblast phenotype. *J. Biol. Chem.* **278**, 50563-50571.

Tseng, D.-Y., Chou, M.-Y., Tseng, Y.-C., Hsiao, C.-D., Huang, C.-J., Kaneko, T. and Hwang, P.-P. (2009). Effects of stanniocalcin 1 on calcium uptake in zebrafish (Danio rerio) embryo. *Am. J. Physiol. Regul. Integr. Comp. Physiol.* **296**, R549-R557.

Varelas, X. (2014). The Hippo pathway effectors TAZ and YAP in development, homeostasis and disease. *Development* **141**, 1614-1626.

Verreijdt, L., Debiais-Thibaud, M., Borday-Birraux, V., Van der Heyden, C., Sire, J.-Y. and Huysseune, A. (2006). Expression of the dlx gene family during formation of the cranial bones in the zebrafish (Danio rerio): differential involvement in the visceral skeleton and braincase. *Dev. Dyn.* **235**, 1371-1389.

von, G. A., Lin, Z., Schlegelmilch, K., Honor, L. B., Pan, G. M., Buck, J. N., Ma, Q., Ishiwata, T., Zhou, B., Camargo, F. D. et al. (2012). YAP1, the nuclear target of Hippo signaling, stimulates heart growth through cardiomyocyte proliferation but not hypertrophy. *Proc. Natl. Acad. Sci. USA* **109**, 2394-2399.

Westerfield, M. (2007). *The Zebrafish Book. A Guide for the Laboratory Used of Zebrafsih (Danio rerio)*, 5th edn. Eugene, USA: University of Oregon Press.

Yang, J.-Y., Cho, S. W., An, J. H., Jung, J. Y., Kim, S. W., Kim, S. Y., Kim, J. E. and Shin, C. S. (2013). Osteoblast-targeted overexpression of TAZ increases bone mass in vivo. *PLoS ONE* **8**, e56585.

Yasoda, A., Komatsu, Y., Chusho, H., Miyazawa, T., Ozasa, A., Miura, M., Kurihara, T., Rogi, T., Tanaka, S., Suda, M. et al. (2004). Overexpression of CNP in chondrocytes rescues achondroplasia through a MAPK-dependent pathway. *Nat. Med.* **10**, 80-86.

Zaidi, S. K., Sullivan, A. J., Medina, R., Ito, Y., van Wijnen, A. J., Stein, J. L., Lian, J. B. and Stein, G. S. (2004). Tyrosine phosphorylation controls Runx2-mediated subnuclear targeting of YAP to repress transcription. *EMBO J.* **23**, 790-799.

Zhang, H., Liu, C.-Y., Zha, Z.-Y., Zhao, B., Yao, J., Zhao, S., Xiong, Y., Lei, Q.-Y. and Guan, K.-L. (2009). TEAD transcription factors mediate the function of TAZ in cell growth and epithelial-mesenchymal transition. *J. Biol. Chem.* **284**, 13355-13362.

Zhao, B., Wei, X., Li, W., Udan, R. S., Yang, Q., Kim, J., Xie, J., Ikenoue, T., Yu, J., Li, L. et al. (2007). Inactivation of YAP oncoprotein by the Hippo pathway is involved in cell contact inhibition and tissue growth control. *Genes Dev.* **21**, 2747-2761.

Zhao, B., Ye, X., Yu, J., Li, L., Li, W., Li, S., Yu, J., Lin, J. D., Wang, C.-Y., Chinnaiyan, A. M. et al. (2008). TEAD mediates YAP-dependent gene induction and growth control. *Genes Dev.* **22**, 1962-1971.

Zhao, B., Li, L., Lei, Q. and Guan, K. L. (2010). The Hippo-YAP pathway in organ size control and tumorigenesis: an updated version. *Genes Dev.* **24**, 862-874.

Zhou, X., Zhang, Z., Feng, J. Q., Dusevich, V. M., Sinha, K., Zhang, H., Darnay, B. G. and de Crombrugghe, B. (2010). Multiple functions of Osterix are required for bone growth and homeostasis in postnatal mice. *Proc. Natl. Acad. Sci. USA* **107**, 12919-12924.

DEVELOPMENT